The Human Interferon- and Estrogen-Regulated *ISG20/HEM45* Gene Product Degrades Single-Stranded RNA and DNA in Vitro†

Lam H. Nguyen,‡ Lucile Espert,§ Nadir Mechti,*,§ and David M. Wilson, III*,‡

Molecular and Structural Biology Division, Lawrence Livermore National Laboratory, P.O. Box 808, L-441, Livermore, California 94551, and U475 INSERM, 99 rue du Puech Villa, 34197 Montpellier Cedex 5, France

Received January 22, 2001; Revised Manuscript Received April 19, 2001

ABSTRACT: The human *ISG20/HEM45* gene was identified independently on the basis of its increased level of expression in response to either interferon or estrogen hormone. Notably, the encoded protein is homologous with members of the 3′ to 5′ exonuclease superfamily that includes RNases T and D, and the proofreading domain of *Escherichia coli* DNA polymerase I. We provide here direct biochemical evidence that Isg20 acts as a 3′ to 5′ exonuclease in vitro. This protein displays a pH optimum of ∼7.0, prefers Mn^{2+} as a metal cofactor, and degrades RNA at a rate that is ∼35-fold higher than its rate for single-stranded DNA. Along with RNase L, Isg20 is the second known RNase regulated by interferon. Previous data showed that Isg20 is located in promyelocytic leukemia (PML) nuclear bodies, known sites of hormone-dependent RNA polymerase II transcription and oncogenic DNA viral transcription and replication. The combined data suggest a potential role for Isg20 in degrading viral RNAs as part of the interferon-regulated antiviral response and/or cellular mRNAs as a regulatory component of interferon and estrogen signaling.

Interferons (IFNs)[1] make up a family of secreted cellular proteins involved in regulating cell proliferation, cellular differentiation, immune response, and the general antiviral response (reviewed in refs *1*−*3*). Estrogen is a hormone that promotes mitogenic responses in a number of cell types, particularly female reproductive tissue (*4*). The *ISG20* (interferon-stimulated gene product of 20 kDa) gene, also called *HEM45* (HeLa estrogen-modulated, band 45), was identified on the basis of transcript induction following exposure to either IFN or estrogen (*4*, *5*). These observations suggested a role for Isg20 in mediating the regulatory and/or developmental activities of such agents.

Isg20, like some other IFN-induced proteins, is located in spherical nuclear particles termed promyelocytic leukemia protein oncogenic domains (PODs) (also known as nuclear domain 10 or the Kr body; reviewed in refs *6* and *7*). PODs are large multiprotein complexes associated with the nuclear matrix (*6*). Although the precise function of these substructures is unknown, certain observations suggest that they may be preferential targets for viral infection and thus could play a mechanistic role in the antiviral action of IFNs (reviewed in ref *7*). In addition, PODs have been implicated in transcriptional regulation (*8*), apoptosis (*9*), maintenance of genomic stability (*10*) and telomere length by a telomerase-independent process (*11*), p53 acetylation, and p53-dependent cellular senescence upon oncogene expression (*12*). Notably, the number and morphology of PODs vary through the cell cycle and in some pathological contexts, including leukemia and viral infections (reviewed in ref *7*).

Recently, Isg20 was placed into the 3′ to 5′ exonuclease superfamily (*13*). This superfamily includes RNases (such as RNase T and D), the proofreading domains of the Pol I family of DNA polymerases, and DNases that exist as independent proteins (such as *Escherichia coli* Exo I) or as domains within larger polypeptides (such as a region within the Werner's syndrome helicase) (*13*−*15*). Homology within the superfamily is concentrated at three conserved exonuclease motifs termed *Exo*I, *Exo*II, and *Exo*III (*13*, *14*). In this report, we present the first biochemical evidence that Isg20 is a 3′ to 5′ exonuclease with a preference for RNA over single-stranded DNA.

EXPERIMENTAL PROCEDURES

Buffers and Reagents. All reagents were purchased from Sigma unless otherwise indicated. Restriction enzymes were purchased from New England Biolabs. Labeled nucleotides were from Amersham. Spectrophotometric-grade glycerol was obtained from Fisher. pET vectors were from Novagen (Madison, WI). DNA oligos were obtained from Operon Biotechnologies (Alameda, CA). Synthetic RNA was obtained from Dharmacon Research (Boulder, CO). L buffer (lysis buffer) contains 50 mM Tris-HCl (pH 7.0), 50 mM NaCl, 20% glycerol, 20 mM β-mercaptoethanol, and 1 mM phenylmethanesulfonyl fluoride (PMSF). W5 buffer is 50 mM Tris-HCl (pH 7.9), 500 mM NaCl, 20% glycerol, 5 mM

† This work was carried out under the auspices of the U.S. Department of Energy by Lawrence Livermore National Laboratory under Contract W-7405-ENG-48 and supported by U.S. Army US-AMRMC (BC980514) and NIH (CA79056) grants to D.M.W. L.E. and N.M. are supported by grants from the Association pour la Recherche contre le Cancer, the Ligue Contre le Cancer, the Federation pour la Recherche Medicale, and the INSERM and CNRS.

* To whom correspondence should be addressed. D.M.W.: e-mail, wilson61@llnl.gov; phone, (925) 423-0695; fax, (925) 422-2282. N.M.: e-mail, mechti@montp.inserm.fr; phone, 04-67-63-62-71; fax, 04-67-04-18-63.

‡ Lawrence Livermore National Laboratory.

§ U475 INSERM.

[1] Abbreviations: IFN, interferon; PML, promyelocytic leukemia; POD, promyelocytic leukemia protein oncogenic domain; PMSF, phenylmethanesulfonyl fluoride.

10.1021/bi010141t CCC: $20.00
Published on Web 05/19/2001

imidazole, 10 mM β-mercaptoethanol, and 1 mM PMSF. W20 is identical to W5, but with 20 mM imidazole. E250 buffer is identical to W5 except it contains 250 mM NaCl and 250 mM imidazole. All pH values were determined at 21 °C.

Purification of Recombinant Isg20 Proteins. To generate pIsg20-His, the *ISG20* coding region was PCR amplified using primers NCO5′ (5′-GCATGCCATGGCTGGGAGC-CGTGAG-3′) and 3′XHO (3′-CGAGTCTCGAGGTCTGA-CACAGCCAGG-5′), partially digested with *Nco*I and *Xho*I, and subcloned into these sites of pET28a (Novagen). This construct allows for expression of a carboxyl-terminal six-histidine-tagged Isg20 fusion protein under the control of the T7 RNA polymerase promoter. To generate a pIsg20D94G plasmid that expresses a D94G (located within the *Exo*II exonuclease motif; *13*) histidine-tagged mutant protein, a 145 bp *Pst*I fragment containing this mutation was gel isolated from the *Pst*I-digested pGST-Isg20ExoII plasmid (see below) and subcloned into the internal *Pst*I sites of pIsg20-His.

The pGST-Isg20 was generated by first PCR amplifying the *ISG20* cDNA coding region with GST 5′ (5′-GTC GGA ATT CAA CTC GAG ATG GCT GGG AGC CGT-3′) and GST 3′ (5′-ACG GTC GAA TTC TAG AGA AAA TAT AGA GCC-3′). The PCR product was then subcloned into the *Eco*RI site (underlined above) of pGEX2T (Amersham/Pharmacia) in the same open reading frame as the GST domain. Site-specific mutants were created using the procedure of the QuickChange Site-Directed Mutagenesis Kit (Stratagene). The following primer sets were employed for PCR amplification (the mutated codon is underlined): for the D11G mutation in the *Exo*I motif, EXO IA (5′-GAG GTG GTG GCC ATG GGC TGC GAG ATG GTG GGG CTG GGG-3′) and EXO IB (5′-CCC CAG CCC CAC CAT CTC GCA GCC CAT GGC CAC CAC CTC-3′); for the D94G mutation in the *Exo*II motif, EXO IIA (5′-CAT GAC CTG AAG CAC GGC TTC CAG GCA CTG AAA GAG GAC-3′) and EXO IIB (5′-GTC CTC TTT CAG TGC CTG GAA GCC GTG CTT CAG GTC ATG-3′); and for the D154G mutation in the *Exo*III motif, EXO IIIA (5′-CAC AGC TCG GTG GAA GGT GCG AGG GCA ACG ATG-3′) and EXO IIIB (5′-CAT CGT TGC CCT CGC ACC TTC CAC CGA GCT GTG-3′). Appropriate PCR products were subsequently cloned into the pGST-Isg20 to generate pGST-Isg20*Exo*I, pGST-Isg20*Exo*II, and pGST-Isg20*Exo*III.

To generate the His-tagged Isg20 protein, pIsg20-His was transformed into the BL21(DE3)/pLysS *E. coli* strain (Novagen). An overnight culture of 100 mL was subsequently grown at 37 °C in LB (1% bacto-tryptone, 0.5% bacto-yeast extract, and 1% NaCl) with 30 μg/mL kanamycin and 25 μg/mL chloramphenicol. The overnight culture was used to inoculate 2 L of the same medium. This culture was grown at 37 °C with vigorous aeration until the A_{550} was ~0.6. Isopropyl 1-thio-β-galactopyranoside was then added (final concentration of 1 mM) to induce Isg20-His protein expression. After induction for 4 h, cells were harvested, and cell pellets were frozen at −20 °C. Notably, the pIsg20-His plasmid, but not the pIsg20D94G plasmid, causes a 2−3-fold decrease in the rate of growth of BL21(DE3) cells (in the uninduced state and with the pLysS plasmid; data not shown), suggesting that the nuclease activity of Isg20 reduces the growth rate. The cell pellet was thawed and resuspended in 30 mL of L buffer. The cell suspension was sonicated using a Misonix XL sonicator with a macrotip at the maximum setting with two 1 min bursts. The cell lysate was centrifuged at 27000*g* for 30 min at 4 °C. To the supernatant was added slowly polyethyleneimine with constant stirring to a final concentration of 0.3% to remove nucleic acids (*16*). The suspension was centrifuged, and to the supernatant were added NaCl and imidazole to final concentrations of 500 and 5 mM, respectively. The soluble protein extract was then incubated with 2 mL of Ni−NTA resin (Qiagen, Santa Clarita, CA) for 1 h at 4 °C with gentle rocking. This suspension was centrifuged, and the resin was washed two times each with 20 mL of W5 buffer, followed by two washes each with 20 mL of W20 buffer. Isg20-His proteins were then eluted from the Ni−NTA resin four times, each with 2 mL of E250 buffer. These eluants were pooled. Imidazole was removed by two rounds of concentration with Centricon 30 concentrators and dilution with L buffer containing 0.1 mM DTT. Glycerol was then added to the retentate to a final concentration of 50%, and these protein samples were stored at −20 °C, as Isg20-His appears to be sensitive to multiple freeze−thaw cycles. Under such storage conditions, Isg20-His is stable for ~3 months. Concentrations of protein solutions were determined by measuring the absorbance at 280 nm and using the theoretical molar extinction coefficient E_{280} of 13 325 M^{-1} cm^{-1} calculated for Isg20-His (*17*). From 2 L of induced bacterial culture, we obtained ~0.5 mg of Isg20-His fusion protein. GST-Isg20, GST-Isg20*Exo*I, GST-Isg20*Exo*II, and GST-Isg20*Exo*III fusion proteins were generated and partially purified according to the protocol of Pharmacia.

Nuclease Assays. Various DNA and RNA substrates were labeled at the 5′ end with T4 polynucleotide kinase and [γ-^{32}P]ATP (*18*). RNA5 is 5′-GAUCG-3′. DNA5 is 5′-GATCG-3′. Supercoiled pET-28a was used as the promoter DNA template to produce a 343-nucleotide RNA with a 15-base stem and 6-base loop structure (TΦ transcription terminator) at the 3′ end (*19*). For the 210-nucleotide RNA, the transcription template was the pET-28a plasmid linearized with *Xho*I, a restriction enzyme that cuts specifically between the T7 promoter and the TΦ transcription terminator. Uniformly labeled RNA substrates were synthesized with T7 RNA polymerase and [α-^{32}P]GTP according to the instructions of the manufacturer (Gibco-BRL).

Labeled nucleic acid substrate (200−400 fmol) was incubated with 40−1000 fmol of Isg20-His protein at 37 °C in 10 μL of 50 mM HEPES-KOH (pH 7.0) 10% glycerol, 50 mM NaCl, 1 mM $MnCl_2$, 0.01% Triton X-100, and 1 mM DTT. The reactions were stopped with 10 μL of an 80% formamide dye solution, and the mixtures were heated at 80 °C for 3 min and then fractionated on a 20 or 22.5% urea (8 M)−polyacrylamide gel. Visualization of the labeled substrate and product was achieved using a Molecular Dynamics (Sunnyvale, CA) STORM 860 Phosphorimager, and quantitative analysis was performed using Molecular Dynamics ImageQuant version 1.11 software. For the pH titrations, instead of 50 mM HEPES-KOH (pH 7.0), different pHs were obtained using a buffer mixture of constant ionic strength consisting of 25 mM acetic acid and MES, and 50 mM Trizma base (*20*). Specific activity is defined as units per microgram of Isg20-His, with 1 unit being 1 pmol of RNA5 or DNA5 substrate degraded to mononucleotides in 1 min at 37 °C.

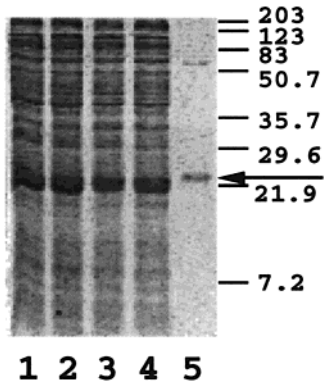

FIGURE 1: Isg20-His protein. Aliquots of protein fractions from the various purification steps separated on a 15% polyacrylamide−SDS gel: lane 1, whole cell extract; lane 2, whole cell supernatant; lane 3, 0.3% polyethyleneimine supernatant; lane 4, flow-through from Ni affinity chromatography; and lane 5, Ni affinity-purified fraction. Sizes of protein standards are indicated in kilodaltons on the right. The gel was stained with Coomassie Blue R250. The arrow indicates the position of Isg20-His.

To search for potential inhibitory effects of the three GST-Isg20 mutant proteins (D11G, D94G, or D154G), 0.1 nM RNA5 was preincubated on ice for 20 min with either of the mutants at 1 nM. Subsequently, 0.05 nM WT Isg20-His protein (which by itself degrades ~100% of the RNA5 substrate) was added to the mutant-containing reaction mixtures and the mixture incubated at 37 °C for 10 min. RNA5 degradation was then evaluated as described above.

RESULTS

Isg20 Is a 3′ to 5′ Exonuclease. The *ISG20* cDNA encodes a 181-amino acid protein of 20 363 Da with a theoretical pI of 9.5. This protein belongs to the 3′ to 5′ exonuclease superfamily (*13*) based on the presence of the three characteristic *Exo*I, -II, and -III motifs (*14*). To examine experimentally the possibility of nuclease activity, the *ISG20* gene was subcloned into the pET28a plasmid to produce a C-terminally tagged Isg20-His fusion protein. The recombinant protein was partially purified as described in Experimental Procedures (Figure 1). As shown in Figure 2 A, this Isg20-His preparation degraded RNA5, DNA5, and the single-stranded region of a 3′ DNA flap, stopping at the double-stranded DNA junction. Isg20-His was ~35-fold more active on single-stranded RNA than DNA (Figure 2A), with a specific activity of 4.21 ± 0.80 units/μg for RNA5 and 0.12 ± 0.01 unit/μg for DNA5. We observed degraded 4-mer products prior to detecting mononucleotides during the time course experiments with both substrates (Figure 2A), consistent with a 3′ to 5′ exonuclease activity.

To determine if the observed DNase and RNase activities are intrinsic to Isg20, particularly in light of the ~65 kDa contaminating band seen in Figure 1, a mutant in a presumed catalytic residue was constructed to obtain an inactive protein. Aspartate 94 of Isg20 was selected because an aspartate to alanine mutation at the structurally equivalent residue in *E. coli* DNA polymerase I causes a significant decrease in its 3′ to 5′ exonuclease activity (*21*). When compared to the wild-type protein, the Isg20D94G mutant (purified using the same procedure; see Experimental Procedures) displayed a >90% reduction in specific activity to degrade RNA5 and DNA5 substrates (Figure 2B). Moreover, a GST-Isg20 fusion

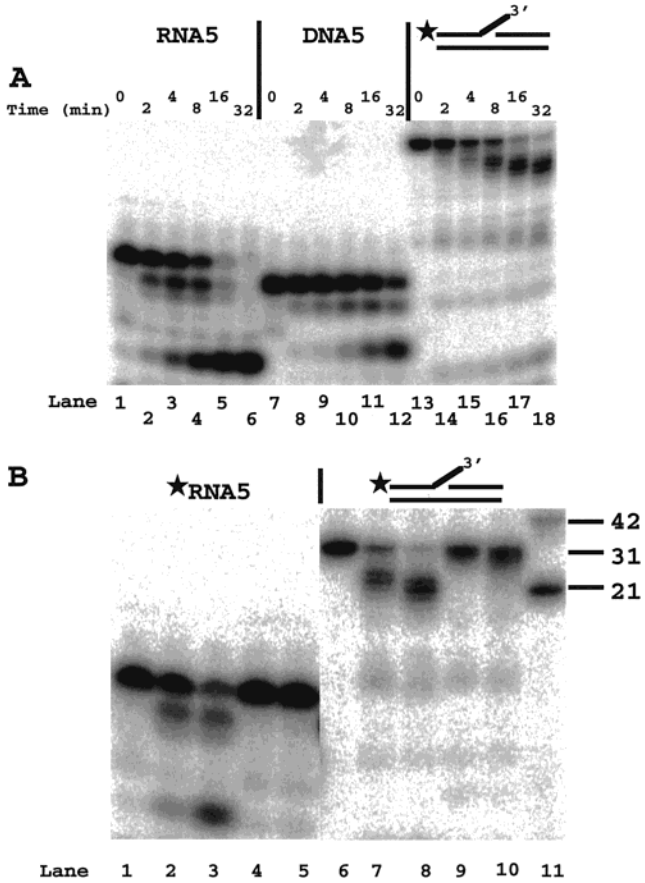

FIGURE 2: Isg20-His is a 3′ to 5′ exonuclease. (A) Isg20-His degrades single-stranded RNA and DNA. RNA5 (40 nM) or a DNA substrate, DNA5 or 3′ flap (40 nM), was incubated with 20 or 200 nM Isg20-His protein, respectively, for various times at 37 °C. RNA5, DNA5, and the strand containing the flap (as indicated by the star) were labeled at the 5′ end. The 3′ flap DNA substrate is described in ref *23*. Lanes 1−6 show reactions performed with RNA5; lanes 7−12, DNA5; and lanes 13−18, 3′ flap DNA substrate of 42 nucleotides in length with a 10-nucleotide flap. Lanes 1, 7, and 13 are the no protein controls; lanes 2, 8, and 14, 2 min incubations with Isg20-His; lanes 3, 9, and 15, 4 min incubations; lanes 4, 10, and 16, 8 min incubations; lanes 5, 11 and 17, 16 min incubations; and lanes 6, 12, and 18, 32 min incubations. (B) The D94G mutation abolishes the DNase and RNase activities of Isg20-His. Lanes 1−5 are the RNA5 (40 nM) reactions, and lanes 6−10 are with the 3′ flap substrate (40 nM). Reactions were performed at 37 °C for 20 min. Lane 1 is RNA5 untreated control. Lanes 2 and 3 correspond to RNA5 incubated with 5 and 15 nM wild-type Isg20-His (WT), respectively. Lanes 4 and 5 correspond to RNA5 incubated with 5 and 15 nM Isg20-D94G (D94G mutant), respectively. Lane 6 corresponds to the 3′ flap DNA undigested control. Lanes 7 and 8 correspond to 50 and 150 nM WT enzyme, respectively. Lanes 9 and 10 correspond to 50 and 150 nM D94G mutant, respectively. Lane 11 contains 42-nucleotide and 21-nucleotide DNA markers. The data presented here are representative of three independent experiments.

protein exhibited RNase and DNase activities similar to that of wild-type Isg20-His (under slightly different in vitro conditions), and site-specific mutations of D11G (in the *Exo*I motif), D94G (*Exo*II), and D154G (*Exo*III) in the GST fusion led to ≥85, ≥87, and ≥87% reductions, respectively, in RNase activity. These data are consistent with both nuclease activities being intrinsic to Isg20, and indicate the importance of these conserved residues. Notably, nucleases that are not members of the 3′ to 5′ exonuclease superfamily, specifically, human Ape1 (an abasic endonuclease of the *E. coli* exonuclease III family; *22*), *E. coli* endonuclease IV (a representa-

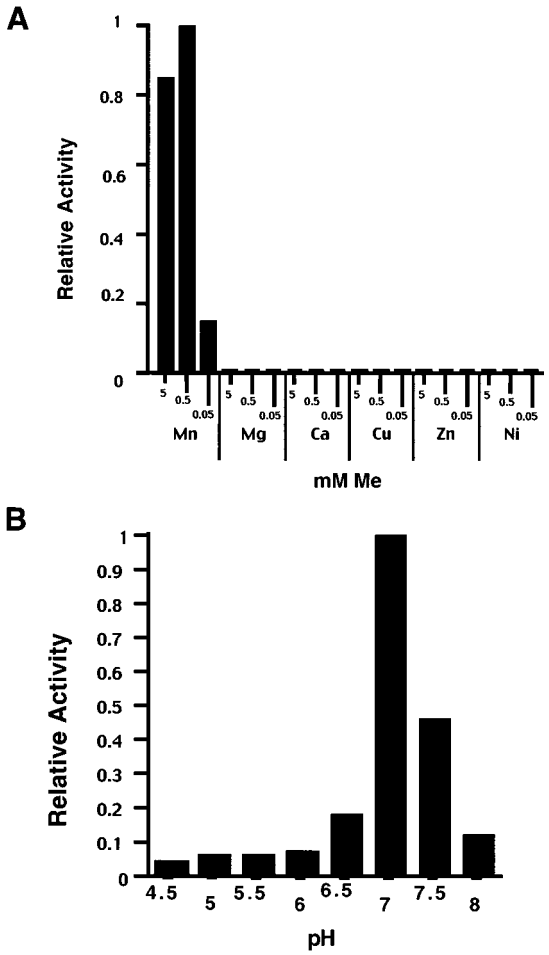

FIGURE 3: Metal cofactor requirement and pH optimum of Isg20-His exonuclease activity. (A) Metal cofactor requirement. The labeled RNA5 substrate (40 nM) was incubated with 2 nM Isg20-His enzyme for 10 min at 37 °C with different concentrations (5, 0.5, and 0.05 mM) of the various divalent metal cations, with chloride as the anion. Exonuclease activity is represented by the amount of labeled RNA5 substrate converted to the final mononucleotide product. The highest activity was designated as 1. At all the concentrations tested here, the relative activity was <0.01 for $MgCl_2$, $CaCl_2$, $CuCl_2$, $NiCl_2$, and $ZnCl_2$. Shown is a representative of three independent experiments. (B) pH optimum. 5′-labeled RNA5 (40 nM) was incubated with 2 nM Isg20-His for 10 min at 37 °C at the various pHs. The pH was maintained with a mixture of 25 mM acetic acid, 25 mM MES, and 50 mM Tris-HCl (*20*). The relative exonuclease activities were determined as described for panel A.

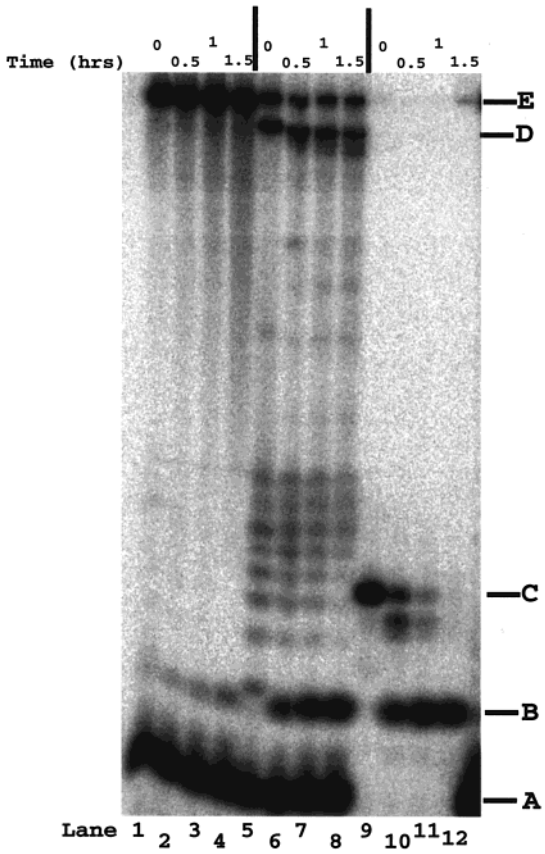

FIGURE 4: Isg20-His nuclease activity on long RNA substrates with or without a stem−loop structure at the 3′ end. Lanes 1−4 are reactions with uniformly labeled 343-base RNA with the TΦ transcription terminator stem−loop structure at the 3′ end, lanes 5−8 uniformly labeled 210-base RNA, and lanes 9−12 RNA5 labeled at the 5′ end. Lanes 1, 5, and 9 are the no protein controls. All the other lanes are reactions with 10 nM Isg20-His. Lanes 2, 6, and 10 are 30 min reactions at 37 °C; lanes 3, 7, and 11, 60 min reactions; and lanes 4, 8, and 12, 90 min reactions. On the right of the figure, band A is unincorporated [α-P^{32}]GTP; band B, Isg20-His degraded mononucleotide products; band C, RNA5 substrate; band D, 210-base RNA; and band E, 343-base RNA with a 3′ end stem−loop structure. The intermediate products observed in lanes 5−8 (including the no protein control) likely represent abortive initiation RNA products obtained with the linearized DNA promoter template, but not the supercoiled promoter template (*29*). Band E in lanes 5−8 is the RNA product generated from residual supercoiled promoter DNA, due to incomplete linearization of the promoter DNA template by *Xho*I.

tive of an independent abasic endonuclease family; *22*), and the human 5′-nucleases Fen1 and Exo1 (members of the RAD2 nuclease family; *23*), did not degrade DNA5 or RNA5 substrates (data not shown). Last, we found that preincubation of any of the three GST-Isg20 mutant proteins (1 nM) with 0.1 nM RNA5 substrate (see Experimental Procedures) inhibited the WT Isg20-His protein RNase activity by ≥90% in vitro, suggesting that these three GST-Isg20 fusion mutants bind the RNA5 substrate effectively and may exhibit dominant-negative effects in vivo.

Optimal Conditions for the Exonuclease Activity of Isg20. Using a 5′ end-labeled RNA5 as the substrate, we determined the divalent metal cation preference of the human Isg20-His protein. At metal concentrations of 0.05, 0.5, and 5 mM, only Mn^{2+} had a stimulatory effect on the exoribonuclease activity of Isg20-His, whereas Mg^{2+}, Ca^{2+}, Cu^{2+}, Zn^{2+}, and Ni^{2+} had virtually no effect (Figure 3A). The DNase activity of Isg20-His, as determined with the 3′ flap DNA substrate used in Figure 2, exhibited the same metal dependence (data not shown). Moreover, the RNase and DNase activities of Isg20-His on RNA5 and 3′ flap DNA substrates, respectively, exhibited the same pH response, with an optimum of ∼7.0 (Figure 3B and data not shown).

Substrate Preference of Isg20. In addition to RNA5, DNA5, and 3′ flap DNA substrates, we examined Isg20-His nuclease activity on longer RNA substrates, with or without a stem−loop structure at the 3′ end. As shown in Figure 4, Isg20-His degrades not only short RNAs, such as RNA5, but also RNAs 210 nucleotides in length. However, the presence of a stem−loop structure at the 3′ end of a long RNA substrate caused a ∼40-fold reduction in RNase activity (Figure 4). Such data are consistent with the above results indicating that Isg20-His degrades RNA in a 3′ to 5′

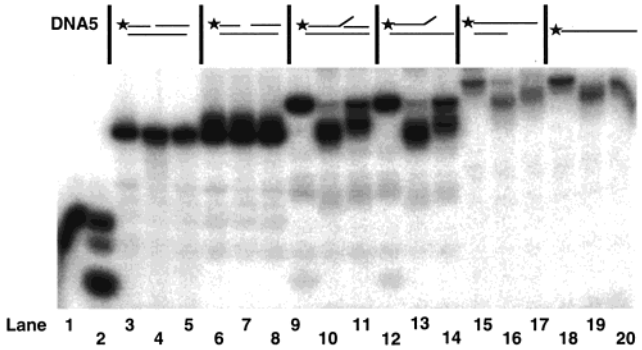

FIGURE 5: DNA substrate preference of Isg20-His. All substrates were labeled at the 5′ end as indicated by the star. Various DNA substrates (shown here and described in ref *23*) at a concentration of 40 nM were incubated with Isg20-His protein for 20 min at 37 °C. Lanes 1, 3, 6, 9, 12, 15, and 18 are the no protein controls. Lanes 1 and 2 are reactions with DNA5; lanes 3−5, nicked DNA; lanes 6−8, one-nucleotide gap DNA; lanes 9−11, 3′ flap DNA; lanes 12−14, 3′ pseudoflap DNA; lanes 15−17, 3′ overhang DNA; and lanes 18−20, single-stranded DNA 42 nucleotides in length. Lanes 2, 4, 7, 10, 13, 16, and 19 are reactions with 256 nM Isg20-His protein, while lanes 5, 8, 11, 14, 17, and 20 are reactions with 64 nM Isg20-His protein.

direction, and operates poorly on double-stranded regions. Results from Figure 4 also suggest that the exonuclease activity of Isg20-His is processive and not distributive on long RNA substrates, since, in a time course, we did not detect any intermediate-sized products between the starting RNA substrate and the final mononucleotide product.

Last, we examined Isg20 nuclease activity on other DNA structures known to be products and/or substrates of DNA repair processes (the various double-stranded DNA substrates used are described in ref *23*). We did not detect significant (<1% of DNA5 specific activity) protein-dependent degradation of 42 bp double-stranded DNAs of 5′ flap, gapped, nicked, or flushed structures (Figure 5 and data not shown). From Figure 5, Isg20 did exhibit weak 3′ to 5′ exonuclease activity (at least 10-fold lower than its RNase activity) on single-stranded DNAs of 42 nucleotides, and the single-stranded DNA regions of 3′ flaps, 3′ pseudoflaps, and 3′ overhangs.

DISCUSSION

We present here biochemical evidence that Isg20 is a 3′ to 5′ exonuclease, with a preference for single-stranded RNA over single-stranded DNA. Notably, Isg20 is the second known RNase regulated by IFN. RNase L, the first IFN-activated RNase, is normally a dormant, cytosolic endoribonuclease. However, upon viral infection or IFN exposure, 2′−5′ oligoadenylate (2−5A) synthetase is activated, increasing the intracellular concentration of short oligoadenylates (reviewed in refs *1*−*3*). These 2−5A oligoadenylates bind RNase L and promote its nuclease activity and, thus in turn, the degradation of cellular 18S and 28S rRNAs as well as viral RNAs, inhibiting cellular protein synthesis and viral propagation. Nevertheless, RNase L (−/−) knockout embryonic fibroblasts are able to develop an IFN-induced antiviral state, suggesting that alternative antiviral mechanisms exist (*24*). Given its localization to PODs, known sites of transcription and replication of oncogenic DNA viruses (e.g., simian virus 40, adenovirus, and herpes simplex virus; *7*), and substrate preferences, the Isg20 protein may act selectively to degrade viral mRNAs as part of an IFN-stimulated antiviral defense mechanism. Such a specialized function is also consistent with the fact that the *Saccharomyces cerevisiae* Isg20 homologue, Rex4p (which is not essential for viability), does not play a prominent role in processing many cellular RNA types (*25*).

The role of the weak DNase activity of Isg20 is less foreseeable. Since it was recently shown that proteins with roles in DNA recombination and telomere maintenance, such as the disease-related proteins Nbs1 and Mre11, are localized to PODs (*10*, *12*), the DNase function of Isg20 may contribute to telomere length maintenance in telomerase-negative immortal cells (*11*).

POD substructures have also been shown to play a role in regulating hormone-dependent transcriptional activity (*26*, *27*). It is conceivable that a function of Isg20, which is induced by estrogen and localized to PODs, is to downregulate the estrogen-dependent transcriptional response by degrading estrogen-induced mRNAs within these substructures. Notably, the estrogen-specific increase in the level of *ISG20* mRNA in immature rat uterus occurs after the enhanced expression of several estrogen early response genes, e.g., c-jun, c-fos, and zif-268 (*4*). Moreover, the downregulation of c-myc expression by IFN occurs through specific degradation of c-myc mRNA (*28*). Future in vivo studies are needed to determine the precise roles of the nuclease activities of Isg20, and the specific contributions of this protein to the cellular IFN-dependent response and the estrogen hormone signaling pathway.

ACKNOWLEDGMENT

We thank Dr. Robert Tebbs for his input.

REFERENCES

1. Lengyel, P. (1993) *Proc. Natl. Acad. Sci. U.S.A. 90*, 5893−5895.
2. Stark, G. R., Kerr, I. M., Williams, B. R., Silverman, R. H., and Schreiber, R. D. (1998) *Annu. Rev. Biochem. 67*, 227−264.
3. Player, M. R., and Torrence, P. F. (1998) *Pharmacol. Ther. 78*, 55−113.
4. Pentecost, B. T. (1998) *Steroid Biochem. Mol. Biol. 64*, 25−33.
5. Gongora, C., David, G., Pintard, L., Tissot, C., Hua, T. D., Dejean, A., and Mechti, N. (1997) *J. Biol. Chem. 272*, 19457−19463.
6. Seeler, J. S., and Dejean, A. (1999) *Curr. Opin. Genet. Dev. 9*, 362−367.
7. Maul, G. G. (1998) *BioEssays 20*, 660−667.
8. Zhong, S., Salomoni, P., and Pandolfi, P. P. (2000) *Nat. Cell Biol. 2*, E85−E90.
9. Guo, A., Salomoni, P., Luo, J., Shih, A., Zhong, S., Gu, W., Paolo, P., and Pandolfi, P. (2000) *Nat. Cell Biol. 2*, 730−736.
10. Lombard, D. B., and Guarente, L. (2000) *Cancer Res. 60*, 2331−2334.
11. Wu, G., Lee, W. H., and Chen, P. L. (2000) *J. Biol. Chem. 275*, 30618−30622.
12. Pearson, M., Carbone, R., Sebastiani, C., Cioce, M., Fagioli, M., Saito, S., Higashimoto, Y., Appella, E., Minucci, S., Pandolfi, P. P., and Pelicci, P. G. (2000) *Nature 406*, 207−210.
13. Moser, M. J., Holley, W. R., Chatterjee, A., and Mian, I. S. (1997) *Nucleic Acids Res. 25*, 5110−5118.
14. Moser, M. J., Holley, W. R., Chatterjee, Bernad, A., Blanco, L., Lazaro, J. M., Martin, G., and Salas, M. (1989) *Cell 59*, 219−228.

15. Joyce, C., and Steitz, T. (1994) *Annu. Rev. Biochem. 63*, 777−822.
16. Burgess, R. R. (1991) *Methods Enzymol. 208*, 3−10.
17. Pace, C. N., Vajdos, F., Fee, L., Grimsley, G., and Gray, T. (1995) *Protein Sci. 4*, 2411−2423.
18. Erzberger, J. P., and Wilson, D. M., III (1999) *J. Mol. Biol. 290*, 447−457.
19. Studier, F. W., Rosenberg, A. H., Dunn, J. J., and Dubendorff, J. W. (1990) *Methods Enzymol. 185*, 60−89.
20. Ellis, K. J., and Morrison, J. F. (1982) *Methods Enzymol. 87*, 405−426.
21. Derbyshire, V., Grindley, N. D., and Joyce, C. M. (1991) *EMBO J. 10*, 17−24.
22. Hadi, M., and Wilson, D. M., III (2000) *Environ. Mol. Mutagen. 36*, 312−324.
23. Lee, B. I., and Wilson, D. M., III (1999) *J. Biol. Chem. 274*, 37763−37769.
24. Zhou, A., Paranjape, J. M., Der, S. D., Williams, B. R., and Silverman, R. H. (1999) *Virology 258*, 435−440.
25. van Hoof, A., Lennertz, P., and Parker, R. (2000) *EMBO J. 19*, 1357−1365.
26. Doucas, V., Tini, M., Egan, D. A., and Evans, R. M. (1999) *Proc. Natl. Acad. Sci. U.S.A. 96*, 2627−2632.
27. LaMorte, V. J., Dyck, J. A., Ochs, R. L., and Evans, R. M. (1998) *Proc. Natl. Acad. Sci. U.S.A. 95*, 4991−4996.
28. Dani, C., Mechti, N., Piechaczyk, M., Lebleu, B., Jeanteur, P., and Blanchard, J. M. (1985) *Proc. Natl. Acad. Sci. U.S.A. 82*, 4896−4899.
29. Diaz, G. A., Rong, M., McAllister, W. T., and Durbin, R. K. (1996) *Biochemistry 35*, 10837−10843.

BI010141T